(Manuscript to *Composite Structures*)

Vibration Design of Laminated Fibrous Composite Plates with Local Anisotropy Induced by Short Fibers and Curvilinear Fibers

Shinya HONDA and Yoshihiro NARITA

Division of Human Mechanical Systems & Design,

Facultyl of Engineering, Hokkaido University

This manuscript has been neither published nor currently submitted for publication either in a serial, professional journal or as a part in a book.

Number of manuscript pages: 21

Number of figures: 9

Number of tables: 2

Mailing address of corresponding author:

Shinya HONDA (Ph.D. in Engineering)

Laboratory of Intelligent Design, Division of Human Mechanical Systems & Design, Faculty of Engineering, Hokkaido University

N13W8, Kita-ku, Sapporo, Hokkaido, 060-8628, Japan

E-mail: honda@eng.hokudai.ac.jp

Tell/Fax: +81-11-706-6416

Vibration Design of Laminated Fibrous Composite Plates with Local Anisotropy Induced by Short Fibers and Curvilinear Fibers

Shinya HONDA*[1] and Yoshihiro NARITA*[2]

*[1] Corresponding Author, Faculty of Engineering, Hokkaido University,

N13W8, Kita-ku, Sapporo, Hokkaido, 060-8628, Japan, honda@eng.hokudai.ac.jp

*[2] Hokkaido University, ynarita@eng.hokudai.ac.jp

[Abstract]

The present paper studies an optimum design method for proposing new types of fiber-reinforced composite plates with locally anisotropic structure. A finite element program is developed to analyze vibration of such locally anisotropic plates, and the fundamental frequency is taken as an object function to be maximized. First, for demonstrating the effectiveness of local anisotropy, the optimum distributions of short fibers are calculated without directional constraints using a simple genetic algorithm (GA), and the layerwise optimization (LO) concept is used to reduce the computation time in the finite element calculation. Secondly, optimum arrangements of continuous curvilinear fibers are obtained under the continuity constraints where fibers directions are considered as projections of contour lines of a cubic polynomial surface. Numerical results show that the local anisotropy successfully improves frequency property and the optimum directions of short fibers indicate physically reasonable orientations. Also, the plates with optimally shaped continuous fibers yield higher fundamental frequencies than the conventional plates with parallel fibers.

***Keywords*:** Local anisotropy, Genetic algorithm, Fiber reinforced composite, Short fiber, Curvilinear fiber, Natural Frequency

1. Introduction

The present paper focuses on locally anisotropic structures which are often found as parts of natural compounds. For example, the bony pelvis of humans is composed of inorganic calcium phosphates and organic collagen fibers. The inorganic component contributes to stiffness and strength, while organic fibers provide toughness. The organic fibers form curvilinear shapes which are possibly the optimum shape to sustain external forces. In other words, the natural compounds have local anisotropic properties distributed optimally throughout the compound to perform more effectively than simple anisotropic materials. It may then be hypothesized that if local anisotropy is exploited in structural design, it will be highly possible to design more effective engineering structures.

To realize local anisotropy with curvilinear fibers, fiber reinforced composites would be highly appropriate, especially with an innovative method that has recently been developed to produce composites with curvilinear fibers. The method is termed automated tow-placement technology [1], and combines features of two conventional methods, i.e., differential tow-payout ability in filament winding, and the compaction and cut-restart capabilities of automated tape laying. The machine head has a wide range of degrees of freedom for axial motion, and the tow-placement direction can be changed continuously. In the fiber placement process, individual prepreg tows are fed with controlled tension and compacted by a heated rolling compaction device onto the lay-up surface.

The mechanical properties of composite plates reinforced by curvilinear fibers strongly depend on the fiber shapes, and such composite plates display non-uniform stiffness and anisotropy. As compared with homogenously anisotropic plates with parallel fibers, there is the potential that task specific fibrous composite plates may be designed using automated tow-placement equipment and curvilinear fibers.

Leissa and Martin [2] first proposed a variable stiffness concept by varying fiber spacings to improve the vibration and buckling performance of plates with the Ritz method. Hyer and Lee [3] employed finite element analysis (FEA) to analyze the buckling performance of plates with variable stiffness formed by curvilinear fibers. Here, the fiber orientation angles between adjacent elements was varied, and it was found that such plates had higher failure loads than plates with parallel fibers. Qatu [4] mentioned curvilinear fibers for circular plates in the polar coordinates. Gürdal et al. [1, 5-7] defined arbitrarily shaped fibers by the linear change in fiber orientation angles between two different reference points for plates and conical shells, and confirmed that such plates have superior mechanical properties compared with homogenous plates by integrated research including experimental and analytical tests. The authors [8] have calculated the natural frequencies of plates reinforced by quadratically shaped fibers using the Ritz method, and showed that plates with local properties have advantages over homogenously anisotropic plates with parallel fibers in terms of vibration design.

For the optimization of locally anisotropic composites, Setoodeh et al. [9-11] studied the optimization of plates with local properties by employing lamination parameters which describe laminated plate properties in simple form as design variables. Blom et al. [12] designed conical shells using curvilinear fibers for maximizing fundamental frequencies while imposing manufacturing constraints. Cho and Rowlands [13] and Huang and Haftka [14] designed fiber directions to reduce stress concentrations around circular holes. Parnas et al. [15] applied curvilinear fibers to a minimum weight design. Mu and Ulatoska [16] used Ritz method and approximated both displacement vectors and fiber shapes by unknown coefficient and trigonometric function. They gave improved bending stiffnesses for simply supported plates with curvilinear fibers. However, so far no paper has dealt with designs considering optimization of plate vibration with continuous curvilinear fibers for various boundary conditions.

There are a number of papers discussing optimization for laminated composite plates with parallel fibers. Adari and Verijenko [17] determined a minimum cost design of hybrid laminated plates subject to constraints on the fundamental frequencies or separation of frequencies using discrete sets of specified ply angles as a linear optimization problem. Miki et al. proposed a graphic method (described in [18]) introducing a feasible region of two lamination parameters. Fukunaga et al. [19-21] optimized lamination parameters by a gradient method and then derived optimum stacking sequences from corresponding lamination parameters by exploiting geometrical features of such feasible regions. Grenestedt [22] and Serge [23] also determined optimum stacking sequences using a graphic method. Todoroki et al. [24-26] combined a genetic algorithm (GA) with a fractal branch-and-bound method and a response surface approximation, and optimized laminated plates by assigning lamination parameters as design variables. Kameyama and Fukunaga [27] also used GA with lamination parameters and designed aircraft wings of composite plates. Autio [28] applied GA methods to determine corresponding lay-ups to the optimum lamination parameters. In these methods, the GA does not require the implementation of a structural analysis and successfully reduces calculation times when compared with conventional GA approaches which directly assign fiber orientation angles to design variables. Abouhamze and Shakeri [29] optimized laminated cylindrical panels using a GA and neural networks. Paluch et al. [30] studied the optimization of plates with variable thicknesses. Narayana et al. [31] investigated minimum weight designs using a failure mechanism based on failure criteria. Almeida and Awruch [32] introduced special operators in the GA and performed multi-objective optimizations to minimize weight of plates and maximize transverse stiffnesses.

The present work designs optimal locally anisotropic structures of the fibrous laminated composites. First, it aims to confirm the effectiveness of local anisotropy in composite materials by exploring the optimum short fiber distribution without directional constraints on fiber orientations (Problem 1). For determining short fiber

distributions, this study uses a GA which considers fiber angles as the direct design variable in each element in an FEA. The plate generated with the present results display better performance than plates with parallel fibers in terms of fundamental frequencies, and show regular trends in the fiber distribution. After showing the superiority of composites with local anisotropy induced by short fiber distribution optimization, an optimum curvilinear fiber shape is developed under continuous constraints on the fiber orientations, where the fiber shapes are expressed as projections of contour lines on a cubic polynomial surface (Problem 2). The results show that plates with curvilinear fibers also result in higher fundamental frequencies than plates with parallel fibers. Further, the results of both sets of optimizations show that there are specific optimum fiber orientations along the plate boundaries.

2. Analysis and Optimization Procedure

2.1 Optimization of the Short Fiber Distributions (Problem 1)

The assignment of fiber orientation angles as a design variable causes a rapid increase in the number of design variables when adding stacked layers, and layerwise optimization (LO) ideas [33-35] are used with GA to save computational effort, applying sequentially from the outer to the inner layers. This reduces the multi-layer optimization problem to a number of iterations of a single-layer optimization problem.

The discussion here considers a laminated plate with a symmetric K-layer as shown in Fig. 1, where the plate dimensions are given by $a \times b \times h$ (thickness) in an O-xyz co-ordinate system. In each layer, the fiber direction and the direction normal to the fibers for the curved fibers are denoted by 1 and 2, respectively. The plates in the present study are limited to plates that are symmetric around the center of the plate, and there is no coupling between bending and stretching.

To exploit a locally anisotropic plate with the maximum fundamental frequency, an optimum short fiber distribution is first determined. The fiber orientation angle for each element of the FEA in each layer is assigned as the design variable, allowing the present optimization problem to be stated as follows.

$$\begin{aligned} &\text{Maximize}: \Omega_1 \\ &\text{Design variables}: [\theta_1^{(n)} / \theta_2^{(n)} / ... / \theta_{K/2}^{(n)}]_s \quad (n = 1, 2, ..., ne) \\ &\text{Subject to}: -90° < \theta_i^{(n)} \le 90° \quad (i = 1, 2, ..., K/2) \end{aligned} \tag{1}$$

where $\theta_i^{(n)}$ is the angle of the *n*th element in *i*th layer, *ne* is the number of elements, and Ω_1 is the normalized fundamental frequency referred as the frequency parameter

$$\Omega_1 = \omega_1 a^2 \sqrt{\frac{\rho}{D_0}} \tag{2}$$

where $D_0 = E_2 h^3/12(1-\nu_{12}\nu_{21})$ is the reference stiffness, ρ is the material density, and ω_1 is the fundamental angular frequency. No artificial constraints are imposed on the fiber orientation angles because the natural distributions of the local anisotropy would be found here.

Since the design variables are assigned to each element of the FEA, this optimization problem has a very large number of possible solutions. For example, when a plate is divided into 10 × 10 elements and 15° increments are used for the optimization in the -90° to 90° range (12 possible angles), the total number of possible solutions is 12^{100} even for a single-layer plate. In addition, the number of possible solutions increases exponentially with increases in the number of layers. To deal with this very large number of combinations, a layerwise optimization (LO) approach is employed to reduce the number of possible solutions.

The LO approach was developed by Narita [33-35] and is based on the physical observation that the outer layer has a greater stiffness effect than the inner layer in the bending of laminated plates and that it therefore has a stronger influence on the vibration behavior of the plate. The optimum conditions for bending vibrations of laminated plates are assumed to be determined by optimizing each layer sequentially from the outermost to

the innermost layer. In the algorithm, the inner layers are initially assumed to have no stiffness but to have the same density as the other layers while the stiffness of the outer layers are being optimized.

The concept of the LO approach successfully reduces the multi-layer optimization to iterations of the single-layer optimization, because the optimization for each layer is repeated sequentially. The algorithm of the LO approach is presented in Fig. 2, and the optimization problem in Eq. (1) can now be re-formulated as

$$\begin{aligned} &\text{Iterate } i = 1 \text{ to } K/2 \\ &\begin{bmatrix} \text{Maximizing}: \Omega_1 \\ \text{Design variables}: \left\{\theta_i^{(1)}, \theta_i^{(2)}, ..., \theta_i^{(ne)}\right\} \end{bmatrix} \\ &\text{Subject to}: -90° < \theta_i^{(n)} \le 90° \end{aligned} \tag{3}$$

Iterations of this optimization starting from the outermost layer of a laminated plate may determine an optimum fiber distribution for each layer, and then, by adding further iterations, a plate with more layers can be optimized. The advantages of the LO approach are to reduce the dimension of calculation for each optimization process and to make it insensitive to increases in the number of layers to be optimized. Moreover, the accuracy is improved by adding a further set of iterations while maintaining fiber orientations from the previous cycle (See Fig. 2 (ii) Second iteration). Due to these repeated processes, the LO approach results in longer calculation times than other approaches optimizing whole layers simultaneously.

2.2. Optimization of the Curvilinearly Shaped Fibers (Problem 2)

Based on the above discussion, optimum curvilinear fiber shapes can be exploited under continuously varying constraints because the optimum short fiber distributions showed specific orientations as will be developed in the following (Section 3.1). To define curvilinearly shaped fibers, a cubic polynomial function $f(x,y)$ is introduced here, as

$$f(x,y) = c_{00} + c_{10}x + c_{01}y + c_{20}x^2 + c_{11}xy + c_{02}y^2 + c_{30}x^3 + c_{21}x^2y + c_{12}xy^2 + c_{03}y^3 \quad (4)$$

where c_{ij} (i, j = 0, 1, 2, 3) are shape coefficients which determine the surface shape. An example of a surface and the corresponding curves is shown in Fig. 3(a) and (b). The expression in Eq. (4) is based on the level set function used in topology optimization and makes it possible to accommodate topology changes simply [36]. In FEA, continuous fibers are discretized and the fiber orientation angles for each element are calculated using the co-ordinates of the center of the element by

$$\theta(x_c, y_c) = \tan^{-1}\left(-\frac{\partial f / \partial x}{\partial f / \partial y}\right)\Bigg|_{x=x_c, y=y_c} \quad \text{(when } \partial f / \partial y = 0,\ \theta = 90^{\circ}\text{)} \quad (5)$$

where (x_c, y_c) are the co-ordinates of the center of the element. The angles are in the same direction as the tangents to the surfaces in the horizontal plane, and assume straight fibers and a constant volume fraction in the element but different angles for each element (Fig. 3(c)). It is possible to describe different shapes of surfaces and curvilinear fibers by varying the values of the shape coefficients. The angle is defined by the continuous polynomial function and this description imposes continuity constraints on the fibers. Further, the present description is more effective and flexible than using the spline function because there is no need to solve simultaneous equations to determine the fiber shapes as it simply accepts the multi-valued functions.

Problem 2 limits plates to symmetric K-angle-ply laminates $[(\pm\theta)_{K/4}]$s where the "+ layer" means that the layer has fiber shapes determined in the optimization problem, and the "- layer" is the layer with fiber shapes symmetric to the "+ layer" with respect to the horizontal line and becomes $-\theta$ in Eq. (5). Thus it is sufficient to design one layer in this problem formulation. The objective is to maximize the fundamental frequency Ω_1, and the corresponding shape coefficients c_{ij} for the optimum fiber shapes are the design variables. This problem can be stated as

$$\begin{aligned} &\text{Maximize}: \Omega_1 \\ &\text{Design variables}: c_{10}, c_{01}, c_{20}, c_{11}, c_{02}, c_{30}, c_{21}, c_{12}, c_{03} \\ &\text{Subject to}: -1 \le c_{ij} \le 1 \quad (i, j = 0, 1, 2, 3) \end{aligned} \tag{6}$$

The c_{00} is eliminated in the derivative process in Eq. (5), and it is not included in the design variables. The increment of c_{ij} is 0.1 in the range from -1 to 1, and there are 21 possible values for each shape coefficient. These values were determined by try and error in the preliminary numerical experiment.

2.3 Genetic Algorithm

For the single layer optimization problem in the optimization of fiber distributions (Problem 1) in Eq. (3) and the optimization of curvilinearlity (Problem 2) in Eq. (6), a genetic algorithm (GA) method coded with an integer representation is employed as an optimizer. Such a GA based on integer coding was used by Riche and Haftka [37], and is commonly used to represent design variables with many possible solutions. When N possible values are considered, an integer ranging from zero to (N-1) is used to represent the possible values.

For GA operators, a two-point crossover and a uniform mutation are used to generate offspring with elitist tactics. Parents with better fitness (frequency parameter Ω_1) are selected by a roulette rule, and the genes (coded by integer parameters) between two crossing points also selected randomly are replaced to generate a child individual in the crossover procedure. In the mutation, a randomly selected gene is converted to another integer with low probability to maintain variety of genes. Further, some of the fittest individuals are selected from the previous generation and used in the next generation where selected individuals are not imposed on the GA operations. This procedure is termed an elitist strategy and is implemented to conserve the gene which may contribute to a better fit and to make the fitness value of the optimization search increase monotonically.

2.4 Finite Element Formulation as Modified in the Present Method

2.4.1 4-node Element Based on the Classical Plate Theory

For the frequency analysis in Problem 1, classical plate theory (CPT) is employed due to its simplicity together with an ACM element as proposed by Adini, Clough and Melosh [38]. An ACM element is rectangular and has 12 degrees of freedom as each corner of the rectangle has three variables (w, $\partial w/\partial x$ and $\partial w/\partial y$). Although this element is a non-confirming element, which may mean that it forms kinks along the boundary between elements, it was confirmed that there are advantages in accuracy and calculation speed because the domain of integration is a simple shape and the integration can be done analytically. The first optimization problem is sensitive to the calculation speed of the structural analysis since the number of design variables is significant and thus a large number of populations and generations have to be included.

For symmetrically laminated thin plates, the maximum strain energy stored in each element is given by

$$U_e = \frac{1}{2}\iint_A \{\kappa\}^T \left[d_{ij}^{(n)} \right] \{\kappa\} \, dA \tag{7}$$

where $d_{ij}^{(n)}$ are the local bending stiffnesses defined by the fiber orientation angles in each element, and $\{\kappa\}$ is a curvature vector obtained by the second derivative of the deflection. The element stiffness matrix $[K_e]$ is obtained from Eq. (7).

The maximum kinetic energy stored in each element is given by

$$T_e = \frac{1}{2}\omega^2 \iint_A \rho w^2 \, dA \tag{8}$$

The element mass matrix $[M_e]$ is obtained from Eq. (8) in the integration process.

The global stiffness matrix $[K]$ and mass matrix $[M]$ are provided by assembling $[K_e]$ and $[M_e]$ for eigenvalue equations. After imposing the boundary conditions on the global matrixes, the frequency parameter is determined by solving an eigenvalue equation.

$$([K]-\omega^2[M])\{\delta\}=0 \tag{9}$$

where $\{\delta\}$ is the global deflection vector.

2.4.2 8-node Element Based on First-order Shear Deformation Theory

For Problem 2, the FEA is performed with an isoparametric eight-node plane element based on the first-order shear deformation theory (FSDT) [39] to enable an analysis of the variously shaped plates. The FSDT is used to consider transverse shear deformation in the frequency analysis, and it does not require continuity in the slope of deflection between element boundaries since the theory is based on a displacement field

$$u=u_0+z\phi_x,\ v=v_0+z\phi_y,\ w=w_0 \tag{10}$$

where (u_0, v_0, w_0) are the displacement of a plane (x, y, 0), and ϕ_x and ϕ_y are the rotations in the x and y directions, respectively. In this paper, laminated plates are limited to symmetric plates (the ply number is K) as shown in Fig. 1, and the in-plane displacements (u, v) are uncoupled from (w, ϕ_x, ϕ_y).

For symmetrically laminated plates, the energy stored in an element of the plate during bending deformation is given by

$$U_{\max}=\frac{1}{2}\int_A\{\kappa_1\}^T\left[d_{ij}^{(n)}\right]\{\kappa_1\}dA+\frac{\alpha}{2}\int_A\{\kappa_2\}^T\left[a_{kl}^{(n)}\right]\{\kappa_2\}dA$$
$$(i,j=1,2,6;\quad k,l=4,5) \tag{11}$$

where $a_{kl}^{(n)}$ are the local shear stiffnesses in the out-of-plane direction of the plate, α is a shear correction factor (= 2 / 3) [40], and the vectors $\{\kappa_1\}$ and $\{\kappa_2\}$ are given by

$$\{\kappa_1\}^T=\left\{-\frac{\partial\phi_x}{\partial x}\quad -\frac{\partial\phi_y}{\partial y}\quad -\left(\frac{\partial\phi_x}{\partial y}+\frac{\partial\phi_y}{\partial x}\right)\right\} \tag{12}$$

$$\{\kappa_2\}^T = \left\{ \frac{\partial w}{\partial x} - \phi_x \quad \frac{\partial w}{\partial y} - \phi_y \right\} \tag{13}$$

The maximum kinetic energy stored in each element during vibration is

$$T_{\max} = \frac{1}{2}\omega^2 \int_A \left(I_1 w^2 + I_3 \phi_x^2 + I_3 \phi_y^2 \right) dA \tag{14}$$

where I_1 and I_3 are inertial amounts given by

$$\left. \begin{aligned} I_1 &= \sum_{k=1}^{2K} \int_{z_{k-1}}^{z_k} \rho dz \\ I_3 &= \sum_{k=1}^{2K} \int_{z_{k-1}}^{z_k} \rho z^2 dz \end{aligned} \right\} \tag{15}$$

After the element stiffness and mass matrices are calculated using a standard routine for FEA with isoparametric elements, the eigenvalue equations are obtained similar to the procedure in Section 2.4.1.

3. Numerical Results and Discussions

Numerical results here were calculated for symmetric 8-layer laminated square plates (a/b = 1 in Fig. 1), with the elastic constants for the graphite/epoxy (CFRP) composite used in the calculations:

E_1 = 138 GPa, E_2 = 8.96 GPa, G_{12} = 7.10 GPa, and v_{12} = 0.3

Figure 4 shows the boundary conditions used in the present study, with letters showing the states of the edges: F for Free, S for simply supported, and C for clamped edges, and the letter P represents a point support. The square plate in Ex. 1 to Ex. 5 are defined with the various boundary conditions of the edges of the plates listed in the counterclockwise direction starting from the left edge of the plate, and all plates are divided into 10 × 10 = 100 elements, thus each plate has 100 design variables in each layer. They present a simply supported plate (Ex. 1 SSSS), a fully clamped plate (Ex. 2 CCCC), a plate with unsymmetrical boundary

conditions including two free edges (Ex. 3 CSFF), a plate with a point support at the free corner of CSFF (Ex. 4 CSF(P)F), and a plate with a mixed boundary at the lower edge (Ex. 5 Mixed S(CS)SS). Ex. 6 is an L-shaped plate with a notch and all edges simply supported. The size of the corner cutout is 0.2*a* with the length of the plate edge *a*, so Ex. 6 has 96 elements for the calculation.

Ex. 7 is a quarter model of a plate with a circular hole at the center of the plate and Ex. 8 is a cantilevered plate imitating the wings (fins) of a rocket. Since only rectangular elements are employed in Problem 1, Ex. 7 and Ex. 8 are not included in the calculations. Plates with finer element divisions than the present also show similar specific orientations (data not shown here), and the 100 element division were employed here in consideration of the calculation effort.

3.1 Results for the Short Fiber Distribution Calculation (Problem 1)

The results from the LO approach are compared with results from conventional GA without LO approach aiming to confirming the efficiency of the LO approach. The conventional GA employs fiber orientation angles in whole layers as design variables. The results are given for the symmetric 8-layer square plates divided into 6 × 6 elements due to saving the calculation time, and boundary condition is all edges clamped since this boundary gives smaller matrices in FEA than others and it is also efficient to save the calculation time. In the present GA, the optimization is carried out each layer sequentially and the number of design variables is 36. On the other hand, the conventional GA has 36 (elements) × 4 (layers) = 144 design variables. Taking the difference of the number of design variables into consideration, the numbers of population are 500 for the present GA and 4000 for the conventional GA. The number of generation is 300 for both GAs. The calculated frequencies are 116. 9 and 107.4 for the present and conventional GAs, respectively, and obtained fiber orientation angles are shown in Fig. 5. The present GA gives higher fundamental frequencies and clearer

fiber orientation than the present GA even the dimension of optimization for GA is smaller. Thus the efficiency of the present approach is confirmed.

The parameters used in the present GA are: number of populations S = 2000, number of generations ge = 500, the crossover probability p_c = 0.7, the mutation p_m = 0.003 and the proportion of elite individuals who are inherited to the next generation without further operation p_e = 0.005. Increment angles of 15° (giving 12 possible angles) are used in this optimization, and the maximum value of the integer used in the integer coding in GA becomes 11 with the first number zero.

Table 1 presents the maximum frequency parameters from the plates calculated here, the values for conventional plates with optimally oriented parallel fibers obtained using the LO method, the optimum lay-ups given by the LO method and the differences (%) based on the values for conventional plates. Table 1 shows that the plates result in higher frequency parameters for all boundary conditions, and it is clearly showing that locally anisotropic plates with optimally oriented short fibers make it possible to design composite plates with higher frequencies than conventional plates.

The optimum short fiber distribution in all layers for the plate with all clamped edges (Ex. 2 CCCC) is shown in Fig. 6, here the outermost layer is defined as the 1st layer. It shows high improvement in frequencies and clear specific fiber orientation in each layer and Ex. 2 is referred here. Figure 7 shows overlapping views for the Exs. 1-6 boundary conditions, with the fibers in the first and second layers shown by bold lines and those in the third and fourth layers with thinner lines.

Figure 6 shows that the fiber placement radiates toward to the center of the plate in the outer two elements adjacent to the plate edges and are oriented concentrically in the inner elements in all layers. These orientations become less distinct in the inner layers, agreeing with the physical observation which the LO concept was based on: the outer layer has a stronger influence to the bending vibration than the inner layers.

The specific fiber orientations are detailed in the overlapping view (Fig. 7, Ex. 2). The fiber orientations are not symmetric in Fig. 5 although the boundary condition is symmetric. This is because GAs are optimization methods based on probabilities and their solutions are not necessarily global-optimum. However, the present solutions result in improved frequencies compared to the conventional plates and they are clear enough to identify tendency in the fiber orientation. The plate has 30.3 % higher fundamental frequency (frequency parameter) than conventional plates, and this improvement is the second largest among the six examples.

The fibers in the simply supported plate (Fig. 7, Ex. 1) form a diamond shape (with two opposing fibers directions at the corners and variety of directions at the center of the elements). In the elements outside the central diamond, fibers are oriented at about 45° and -45°. These angles are the same as in the optimum lay-up of the conventional plate, and here the improvement of 7.22 % is the lowest among the six examples. In Ex. 3, the fibers are oriented horizontally in the elements near the left (clamped) edge, and take on various angles in other elements, giving a 16.4 % improvement in frequency. In Ex. 4 (CSF(P)F), the fibers flow from the lower right corner to the point support (upper right) corner through the center of the plate, and this plate has the largest improvement, 35.7 % compared with the conventional plates. In Ex. 5 with mixed boundary conditions on the lower edge, there are the mixed fiber orientations of Ex. 1 and Ex. 2, giving a 12.7 % improvement in the frequency parameter. The skewed diamond shape orientations due to the corner cut-out appear in Ex. 6, resulting in a frequency that is 9.78 % higher with the shorter fibers.

There is some correlation between the short fiber orientations and the vibration mode. In the vicinity of peaks of vibration modes where the modes have large amplitude and small contour slope, fibers orient concentrically around peaks. Areas adjacent to clamped edges (small amplitude and small contour slope), fibers orient normal to the contour lines of modes, and areas adjacent to simply supported edges (small amplitude and large contour slope), fibers orient ±45º. These characteristics are clear in the Exs. 1 and 2 and

fiber orientations combining both features appear in other examples.

The above discussion allows the conclusion that a plate with optimally distributed short fibers has higher fundamental frequencies than a conventional plate with parallel straight fibers, and that such a plate has specific optimum fiber orientations even when no directional constraints are imposed on the fiber orientation in the design procedure. Regrettably, a material of this kind is not practical with present production techniques and does not satisfy the need for continuity of element boundaries. However, the results suggest the potential for using continuous fibers with optimally curvilinear shapes, and such curvilinear fiber shapes will be determined under the continuity constraint in Problem 2, below.

3.2 Results with the curvilinear fiber calculations (Problem 2)

Problem 2 employs 8-node isoparametric elements (Section 2.1.2) and Ex. 7 and Ex. 8 which have circular edges and trapezoidal elements can also be considered. The GA parameters for Problem 2 are S = 300, ge = 150, pe = 0.9, pm = 0.01 and pe = 0.02.

Figure 3 also discussed in Section 2.2 shows (a) an optimum surface, (b) a model with continuous fibers and (c) a model with the discrete fibers for the totally clamped plate (Ex. 2 CCCC). As suggested by Fig. 3 (a), the surface is described using optimum shape coefficients in *O-xyz* co-ordinates. Figure 3 (b) shows the contour lines projected to the horizontal plane and Fig. 3 (c) presents the discrete model of overlapping of the "+ layer" (bold) with optimized fiber shapes denoted and "− layer" (lighter) with symmetric fiber shapes to the + layer with respect to horizontal line. In the finite element calculation, the fiber orientation of each element is calculated using the co-ordinate of the center of the element based on the surface function (Eq. (5)), and the discrete model is used for the calculation as an approximation of the curvilinear fibers.

Figure 8 suggests the discrete optimum fiber shapes and vibration modes for the eight boundary condition

examples (Fig. 4), where only the "+ layer" is shown as overlapping views would make it difficult to find fiber continuity. The values corresponding to the shape coefficients for Fig. 8 are listed in Table 2, and plots of the fundamental frequencies of the plates here and conventional plates are presented in Fig. 9. The typical 3.lay-up configurations, $[(0^o)_4]s$, $[(0^o/90^o)_2]s$, $[(\pm60^o)_2]s$, $[(\pm45^o)_2]s$ and $[(\pm15^o)_2]s$, are shown in Fig. 9 for comparison.

Except for the purely simply supported plates (Exs. 1 and 6), the plates with curvilinear fibers result in higher frequencies than all conventional plates with typical lay-ups. Even in the case of Exs. 1 and 6, the result is very similar frequencies to the plates with parallel fibers. This is because the optimum fiber shapes for Exs. 1 and 6 show quite similar shapes to $[(\pm45^o)_2]s$ (See Fig. 8, Exs. 1 and 6). The other boundary conditions give clearly curved fiber shapes and higher fundamental frequencies than the parallel fibers.

It is shown by all shapes in Fig. 8 that the fibers respond to the specific shapes along the boundaries and mode shapes. Fibers adjacent to the clamped edges (all edges in Ex. 2, the left edges in Exs. 3, 4 and 8, the left-half of the lower edge in Ex. 5 and the top and right edges in Ex. 7) orient normal to the plate edges, and fibers along the simply supported edges (all edges in Exs. 1 and 6, the lower edge in Ex. 3, and all edges except for the clamped half in Ex. 5) compose $\pm45^o$ shapes. Fibers adjacent to the lower edge in Ex. 4 also meet at an angle. These characteristics, specific to the edges, are very similar to those in the short fiber distribution results (Fig. 7), but no characteristic appears around mode peaks due to continuity constraints.

In Ex. 7, fibers are arranged normal to the circular hole. This is an effect of the clamped edges rather than the hole because when the boundary condition is simply supported, the optimum fibers form a $[(\pm45^o)_2]s$ shape throughout the plate, and they are quite similar to the simply supported plate (Ex. 1). Therefore, the effect on the fiber shapes around a circular hole is small when compared with that of the boundary conditions in terms of fundamental frequencies. However, the amount of improvement for the plate with the circular hole

(Ex. 7) is larger than for the plate without a hole (Ex. 2) as the mass is reduced at the large amplitude area. The wing model (Ex. 8) also shows a specific orientation in elements adjacent to the clamped edge, and fibers orient parallel to the upper edge away from the clamped edge. These shapes are impossible to archive with parallel fibers and are unique characteristics of the curvilinear fibers. Accordingly, it may be concluded that locally anisotropic plates involving curvilinear fibers have higher fundamental frequencies than conventional plates with homogenous anisotropy.

In a previous study [8], it was shown that plates with curvilinear fibers have skewed vibration mode shapes due to the fiber shapes. However the vibration mode shapes indicated in Fig. 8 are not strongly skewed. Thus, the unique mode shapes are not the direct reason for the improvement in the natural frequencies. The improvement of fundamental frequencies for the curvilinear fiber plates (Problem 2) is smaller than for the plates with optimally distributed short fibers (Problem 1). This is because the curvilinear fiber plates have smaller amounts of freedom than the plates with optimally distributed short fibers. Still, curvilinear fibers are simpler realized than the plates with optimally distributed short fibers.

4. Conclusions

To exploit the properties of locally anisotropic structures, the optimum fiber distributions for fibrous composite plates were first determined (Problem 1) in finite elements with independently oriented fibers using a layerwise optimization (LO) idea with a genetic algorithm (GA). The process of the multi-layer optimization of a laminated composite plate was reduced to iterations of optimizations of a single-layer applying the optimization method sequentially from the outermost layer towards to the innermost layer. For the single-layer optimization, each fiber orientation angle in all elements is used as the design variable and optimized simultaneously by the GA. Next, the optimal continuous curvilinear fiber shapes were also found with a GA

(Problem 2). The fiber shapes were denoted by the projections of contour lines for the cubic surfaces, and the coefficients of the cubic polynomial terms were employed as design variables. The finite element analysis (FEA) was used for the vibration analysis, and the fiber orientation angle at each element was calculated from the co-ordinates at the center of element.

In the numerical results for Problem 1, the results of the present approach gave higher fundamental frequencies for all boundary when compared with the fundamental frequencies of conventional plates with parallel fibers. The short fibers were oriented with specific distributions without any constraints, this indicates the possibility to find optimum continuous and curved fiber paths. The results for Problem 2 showed that all the boundary conditions considered here result in higher fundamental frequencies than those of conventional parallel fiber plates with typical lay-ups, except for the purely simply supported square plate. Therefore, it is concluded that the optimum curvilinear fiber shapes determined here give higher or equal fundamental frequencies compared to conventional plates with parallel fibers for the various boundary conditions and that the optimum fiber arrangement is influenced by specific conditions at each boundary condition, but that no specific fiber shape to circular hole was found in this investigation.

Reference

[1] Lopes C. S., Gürdal Z., and Camanho P. P., Variable-stiffness composite panels: Buckling and first-ply failure improvements over straight-fibre laminates, *Computers & Structures* Vol. 86 (2008), pp. 897-907

[2] Leissa A. W. and Martin A. F., Vibration and Buckling of Rectangular Composite Plates with Variable Fiber Spacing, *Composite Structures*, Vol. 14, (1990), pp. 339 – 357.

[3] Hyer M. H. and Lee H. H., The use of curvilinear fiber format to improve buckling resistance of composite plates with central circular holes, *Composite Structures*, Vol. 18 (1991), pp.239-261

[4] Qatu M. S., Vibration of laminated shells and plates, Elsevier Ltd., (2004)

[5] Gürdal Z. and Olmedo R., In-plane response of laminates with spatially varying fiber orientation: variable stiffness concept, *AIAA Journal*, Vol.31, No. 4 (1993), pp. 751-758

[6] Gürdal Z., Tatting B. F., and Wu C. K., Variable stiffness composite panels: effects of stiffness variation on the in-plane and buckling response, *Composites Part A*, Vol. 39, No. 6 (2008), pp. 911-922

[7] Lopes C. S., Camanho P. P., and Gürdal Z., Tatting B. F., Progressive failure analysis of tow-placed, variable-stiffness panels, *International Journal of Solids and Structures*, Vol. 44 (2007), pp. 8493-8516

[8] Honda S., Oonishi Y., Narita Y., and Sasaki K., Vibration analysis of composite rectangular plates reinforced along curved lines, *Journal of System, Design and Dynamics*, Vol. 2, No. 1 (2008), pp. 76-82

[9] Setoodeh S., Abdalla M. M., and Gürdal Z., Design of variable–stiffness laminates using lamination parameters, *Composites Part B: Engineering*, Vol.37(2006), pp.301-309

[10] Setoodeh S., Abdalla M. M., Ijsselmuiden S. T., and Gürdal Z., Design of variable-stiffness composite panels for maximum buckling load, *Composite Structures*, Vol. 87, No. 1 (2009), pp. 109-117

[11] Abdalla M. M., Setoodeh S., and Gürdal Z., Design of variable stiffness composite panels for maximum fundamental frequency using lamination parameters, *Composite Structures*, Vol. 81, No. 2(2007), pp. 283-291

[12] Blom A. W., Setoodeh S., Hol J. M. A. M. and Gürdal Z., Design of variable-stiffness conical shells for maximum fundamental eigenfrequency, *Composite Structures*, Vol. 86 (2008), pp.870-878

[13] Cho H. K. and Rowlands R. E., Reducing tensile stress concentration in perforated hybrid laminate by genetic algorithm, Composite Science and Technology, Vol. 67, 2007, pp. 2877-2883.

[14] Huang J., Haftka R. T., Optimization of fiber orientation near a hole for increased load-carrying capacity of composites, *Structural and Multidisciplinary Optimization*, Vol. 30, pp. 335-341 (2005)

[15] Parnas L., Oral S., and Ceyhan Ü., Optimum design of composite structures with curved fiber courses, *Composites Science and Technology*, Vol. 63 (2003), pp. 1071-1082

[16] Muc A. and Ulatowska A., Design of plates with curved fibre format, *Composite Structures*, Vol. 92 (2010), pp.1728-1733

[17] Adali S. and Verijenko V. E., Optimum stacking sequence design of symmetric hybrid laminates undergoing free vibrations. *Composite Structures*, 54, 131-138 (2001).

[18] Gürdal Z., Haftka R. T. and Hajela P., *Design and Optimization of Laminated Composite Materials*, John Wiley & Sons, London (1999).

[19] Fukunaga H. and Sekine H., Stiffness design method of symmetric laminates using lamination parameters. *AIAA Journal*, 30-11, 2791-2793 (1992).

[20] Fukunaga H., Sekine H., and Sato M., Optimal design of symmetric laminated plates for fundamental frequency. *Journal of Sound and Vibration*, 171, 2, 219-229 (1994).

[21] Fukunaga H, Sekine H., Sato M., and Iino A., Buckling design of symmetrically laminated plates using lamination parameters. *Computers & Structures*, 57, 4, 643-649 (1995).

[22] Grenestedt J. L., Layup optimization and sensitivity analysis of the fundamental eigenfrequency of composite plates. *Composite Structures*, 12, 193-209 (1989).

[23] Serge A., Design of mulitspan composite plates to maximize the fundamental frequency. *Composites Part A: Applied Science and Manufacturing*, 26, 691-697 (1995).

[24] Todoroki A., Haftka R. T., Stacking sequence optimization by a genetic algorithm with a new recessive gene like repair strategy. *Composites Part B: Engineering*, 29, 277-285 (1998).

[25] Todoroki A., Ishikawa T., Design of experiments for stacking sequence optimizations with genetic algorithm using response surface approximation. *Composite Structures*, 64, 349-357 (2004).

[26] Matsuzaki R., Todoroki A., Stacking-sequence optimization using fractal branch-and-bound method for unsymmetrical laminates. *Composite Structures*, 78, 537-550 (2007).

[27] Kameyama M., Fukunaga H., Optimum design of composite plate wings for aeroelastic characteristics using lamination parameters. *Computers & Structures*, 85, 213–224 (2007).

[28] Autio M., Determining the real lay-up of a laminate corresponding to optimal lamination parameters by genetic search. *Structural and Multidisciplinary Optimization*, 20, 301-310 (2000)

[29] Abouhamze M. and Shakeri M., Multi-objective stacking sequence optimization of laminated cylindrical panels using a genetic algorithm and neural networks, *Composite Structures*, Vol. 81 (2007), pp. 253-263.

[30] Paluch B., Grediac M. and Faye A., Combining a finite element programme and a genetic algorithm to optimize composite structures with variable thickness, *Composite Structures*, Vol. 83 (2008), pp. 284-294.

[31] Narayana Naik G., Gopalakrishanan S., and Ganguli R., Design optimization of composite using genetic algorithms and failure mechanism based failure criterion, *Composite Structures*, Vol. 83 (2008), pp. 354-367.

[32] Almeida F. S. and Awruch A. M., Design optimization of composite laminated structures using genetic algorithms and finite element analysis, *Composite Structures*, Vol. 88 (2009), pp. 443-454.

[33] Narita Y., Layerwise optimization for the maximum fundamental frequency of laminated composite plate. *Journal of Sound and Vibration*, 263, 1005-1016 (2003).

[34] Narita Y., Turvey G. J., Maximizing the buckling loads of symmetrically laminated composite rectangular plates using a layerwise optimization approach. *Journal of Mechanical Engineering Science*, 218, 681-691 (2004).

[35] Narita Y., Maximum frequency design of laminated plates with mixed boundary conditions. *International Journal of Solid and Structures*, 43, 4342-4356 (2006).

[36] Allaire G., Jouve F., and Toader A. M, Structural optimization using sensitivity analysis and a level-set method, *Journal of computational physics*, Vol. 194, (2004), pp. 363-393.

[37] Riche L. R. and Haftka R. T., Optimization of laminate stacking sequence for buckling load maximization by genetic algorithm, *AIAA Journal*, Vol. 31 (5), 1993, pp. 951–956.

[38] Zienkiewicz O. C., The finite element method in engineering science 2nd edition, McGraw – Hill, London, 1971.

[39] Reddy J. N., Mechanics of laminated composite plates theory and analysis, CRC Press, Inc., 1997

[40] Whitney J. M. and Pagano N. J., Shear deformation in heterogeneous anisotropic plates, *Journal of Applied Mechanics*, Vol. 37, pp. 1031-1036 (1970)

The number of figures: 9

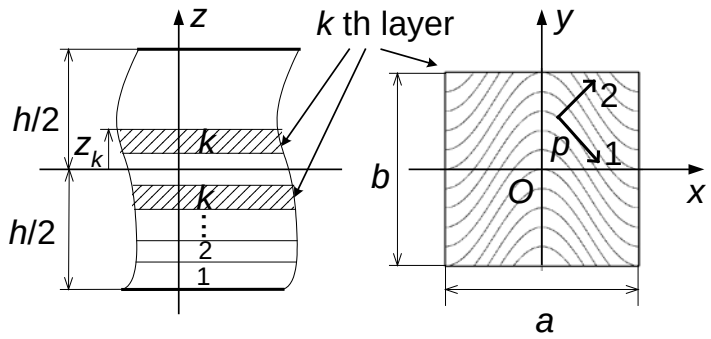

Fig. 1 Cross-section and dimensions of the laminated rectangular plate.

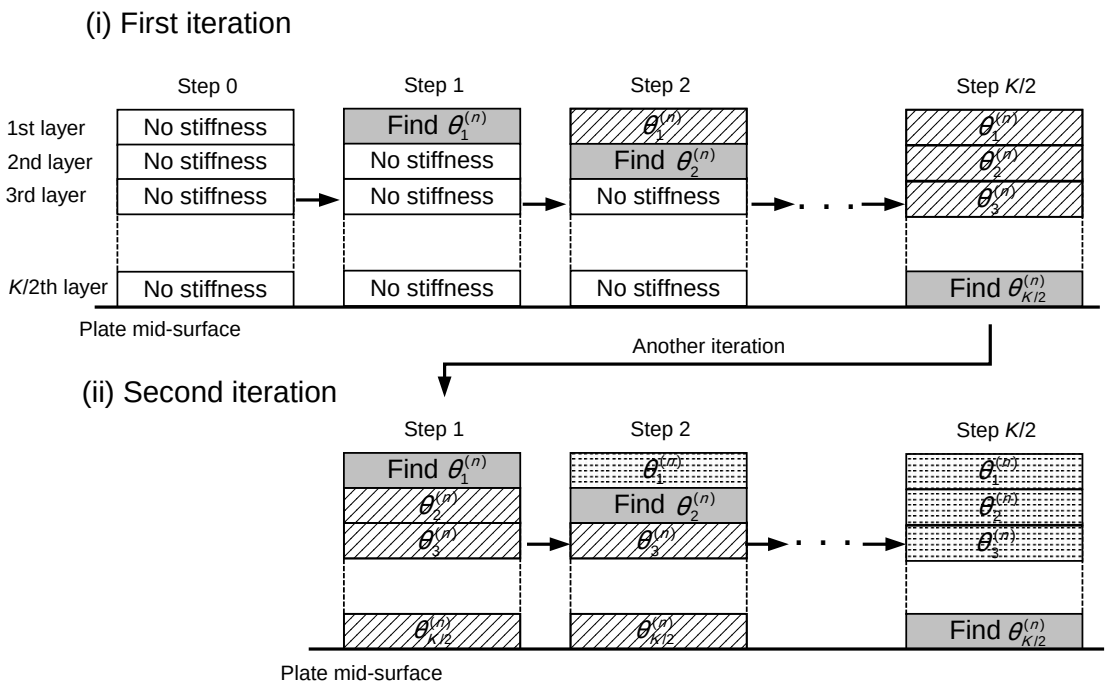

Fig. 2 The process of the algorithm of the LO approach.

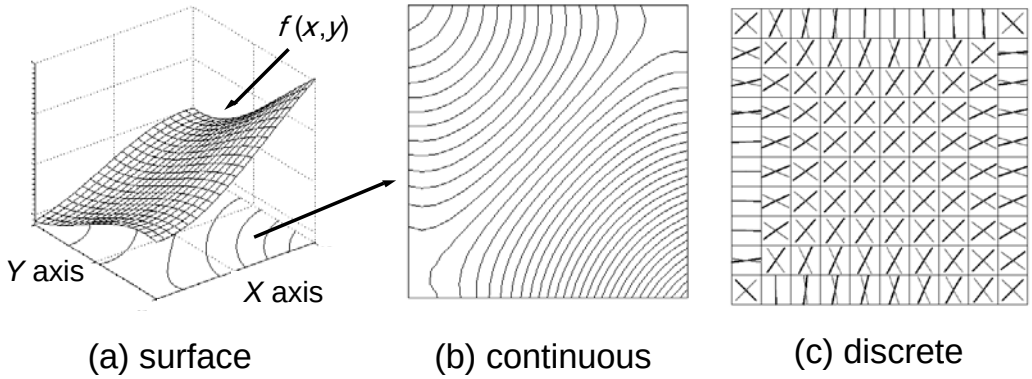

Fig. 3 Examples of (a) surface, (b) continuous fibers and (c) discrete fiber orientaions.

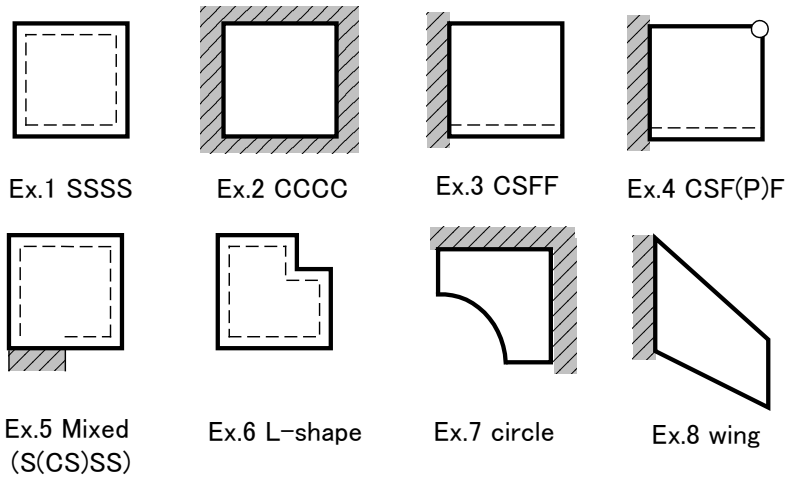

Fig. 4 Boundary condition examples.

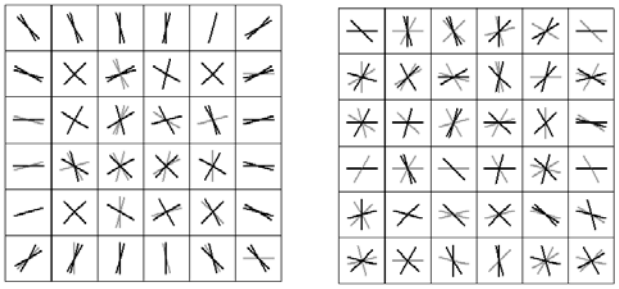

(a) Present GA with LO approch (b) Conventional GA

Fig. 5 Comparison of short fiber distributions between (a) present GA with LO approach and (b) conventional GA

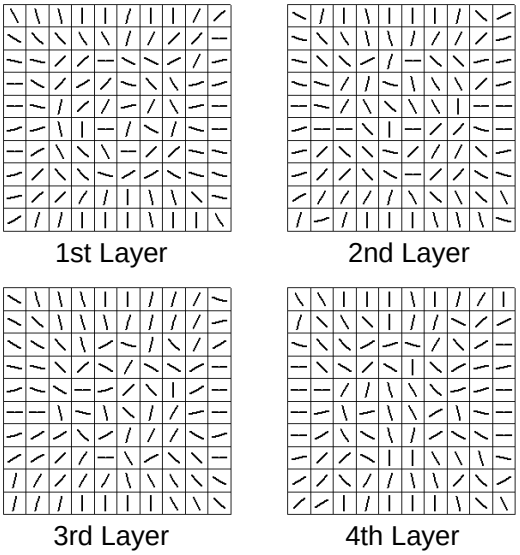

Fig. 6 Optimally distributed short fibers in the layers of a symmetric 8-layer square fully clamped plate (CCCC, Ex. 2).

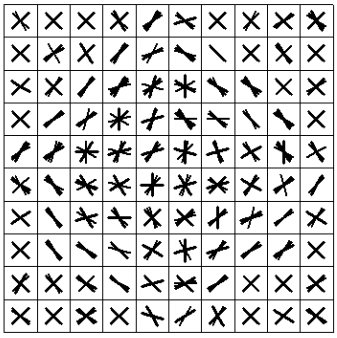

Ex. 1 SSSS

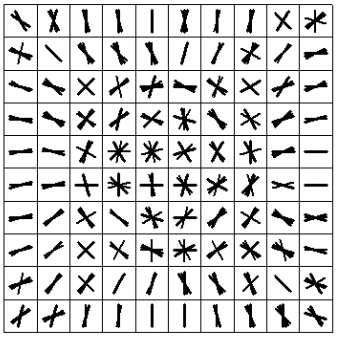

Ex. 2 CCCC

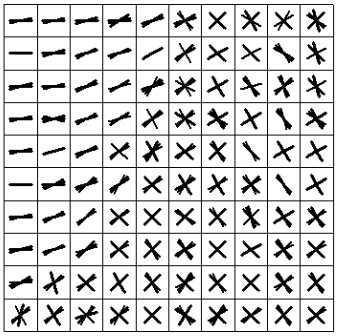

Ex. 3 CSFF

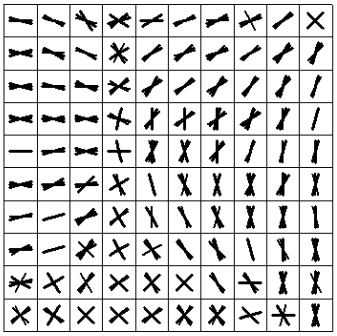

Ex. 4 CSF(P)F

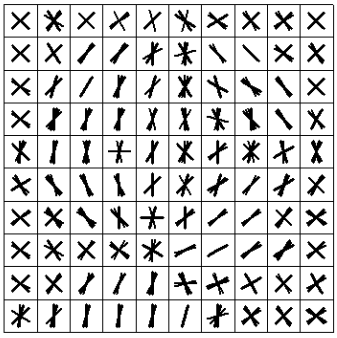

Ex. 5 Mixed (S(CS)SS)

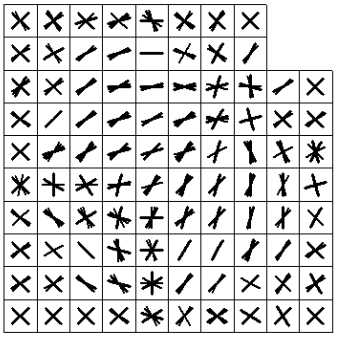

Ex. 6 L-shape

Fig. 7 Overlapping views of the short fiber distributions in the six of boundary conditions (Ex. 1 - 6).

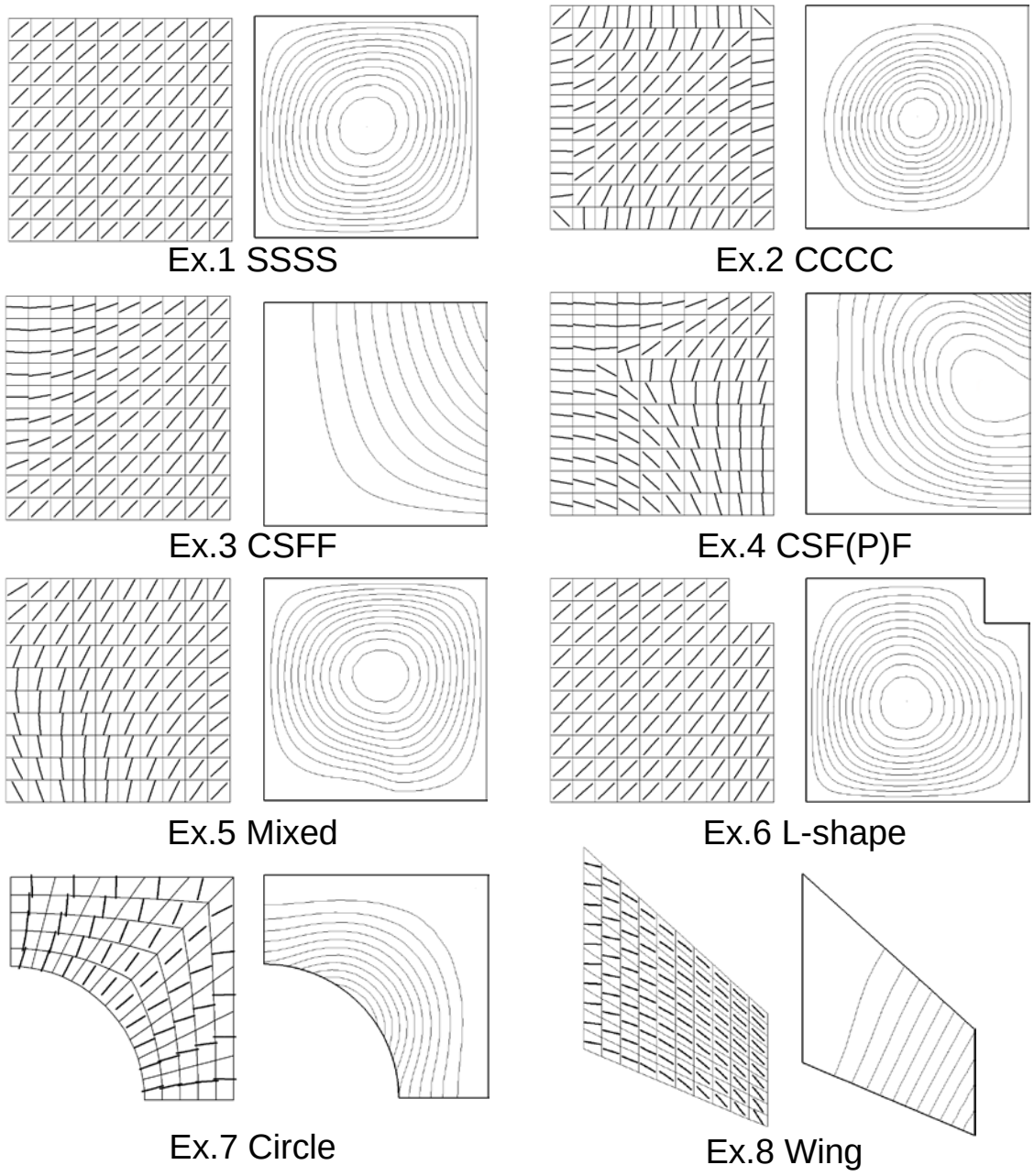

Fig. 8 Discrete models of optimum curvilinear fiber shapes (+ layer) for the eight examples of the plates and the corresponding vibration modes (Ex. 1-8).

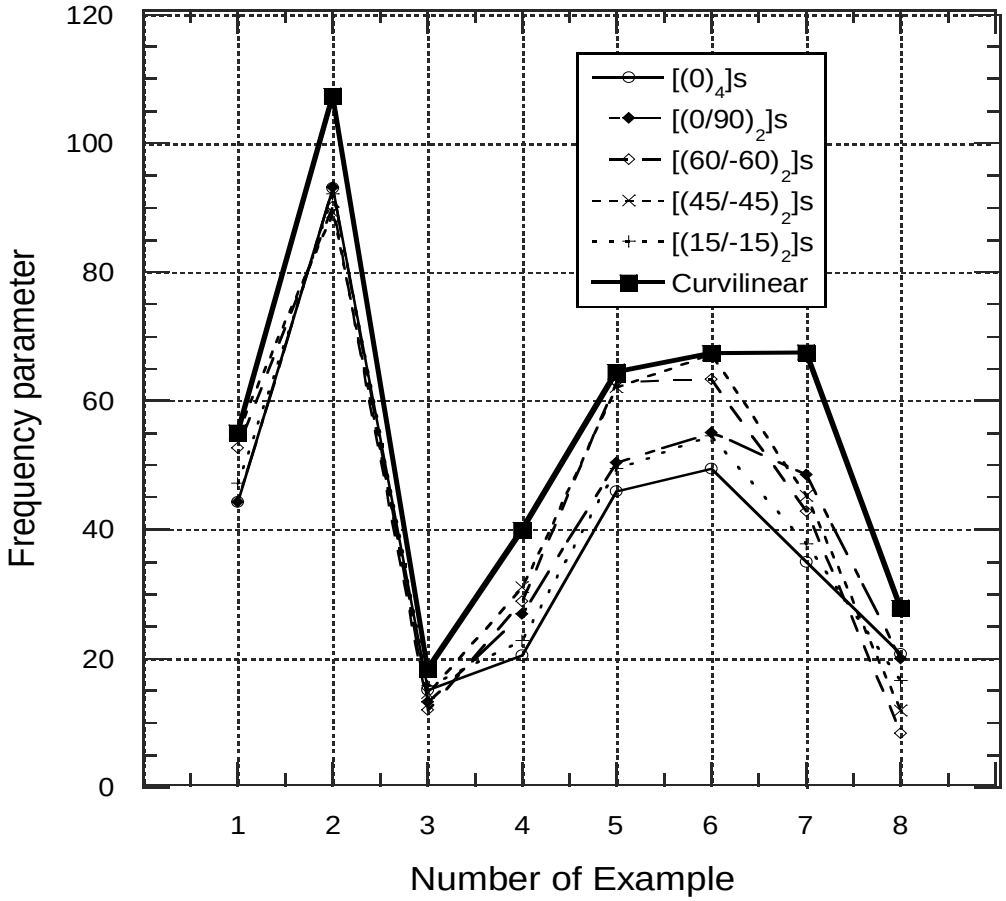

Fig. 9 Frequencies for the present plates with optimum curvilinear fibers and conventional plate with parallel fibers

The number of Tables: 2

Table 1 Maximum frequencies of the present plates and conventional plates, the optimum lay-ups for conventional plates, and differences between frequencies of the plates.

B.C.	Short fiber (dif. %)	Conventional [Opt. Lay-up]
Ex. 1	60.13 (7.22)	56.08 [45/-45/-45/-45]s
Ex. 2	120.9 (30.3)	92.78 [90/0/0/0]s
Ex. 3	19.08 (16.4)	16.39 [20/-45/20/20]s
Ex. 4	43.24 (35.7)	31.87 [55/-50/20/-70]s
Ex. 5	71.48 (12.7)	63.41 [55/-50/-55/55]s
Ex. 6	71.05 (9.78)	64.72 [45/-45/-45/45]s

Table 2 Shape coefficients for the optimum fiber shapes for the eight examples.

BC	(c_{10}, c_{01}, c_{20}, c_{11}, c_{02}, c_{30}, c_{21}, c_{12}, c_{03})
Ex. 1	(1, -0.9, 0.1, 0.1, -0.2, 0.5, -0.9, 0.9, -0.7)
Ex. 2	(0.8, -0.8, 0.2, -0.5, 0.2, -1, -0.9, 1, 1)
Ex. 3	(0.6, -0.8, 0.5, 0.1, -0.6, -0.2, 0.6, 0.5, -0.6)
Ex. 4	(-0.4, -0.3, -0.8, 1, 0.9, -0.8, 0.2, -0.2, 0.5)
Ex. 5	(0.8, -0.4, 0, -0.8, -0.1, -0.5, 0.3, 1, 0.2)
Ex. 6	(1, -0.9, 0.5, -0.3, -0.1, 0.6, -0.6, 0.2, -0.4)
Ex. 7	(-0.9, 0.9, 0.8, 0, -1, 0.2, -0.3, 0.4, 0.1)
Ex. 8	(0.8, 0.9, 0.8, 0.6, 0.1, 0, 1, 0.9, -0.4)